

COMPACT TOROID INJECTION EXPERIMENT IN JFT-2M

T.OGAWA, N.FUKUMOTO¹, M.NAGATA¹, H.OGAWA, M.MAENO, K.HASEGAWA, T.SHIBATA, T.UYAMA¹, J.MIYAZAWA², S.KASAI, H.KAWASHIMA, Y.MIURA, S.SENGOKU, H.KIMURA and JFT-2M Team

Japan Atomic Energy Research Institute, Tokai-mura, Ibaraki-ken, 319-1195 Japan,

¹Himeji Institute of Technology, Himeji, Hyogo, 671-22 Japan,

²National Institute for Fusion Science, Toki, Gifu, 509-52 Japan.

Abstract

Compact toroid (CT) injection experiments with H-mode plasmas were carried out for the first time in JFT-2M. The soft x-ray emission profile shows central penetration of CT in H-mode plasma heated by 1.2 MW NBI as well as in OH plasmas, with toroidal magnetic field of 0.8 T. The line-averaged electron density rapidly increased by $\Delta n_e \sim 0.2 \times 10^{19} \text{ m}^{-3}$ at a rate of $4 \times 10^{21} \text{ m}^{-3}/\text{s}$ in H-mode and the fuelling efficiency was roughly 20%. The asymmetrical radial profile in the soft x-ray emission was produced for $\sim 50 \mu\text{s}$ by the central penetration of CT.

1. INTRODUCTION

Conventional fuelling methods, such as gas puffing and pellet injection in present tokamaks, are considered to be difficult for central fuelling in a fusion reactor, whereas a compact toroid (CT) injection can be expected to make it possible[1]. CT plasma with approximately equal amounts of toroidal and poloidal magnetic fields, can be formed in a magnetized coaxial plasma gun and efficiently accelerated to high velocity[2]. Some promising results on the CT injection were obtained in a few tokamaks[3-5] only in OH plasmas. Himeji Institute of Technology (HIT) developed a CT injector (HIT-CTI) to demonstrate the CT fuelling into H-mode plasmas in the JFT-2M tokamak, whose major and minor radii are 1.31 and 0.35 m in vessel size, respectively. The initial CT injection experiments in JFT-2M, started in November 1997, have been performed with toroidal fields of 0.8 - 1.3 T and plasma currents of 140 - 240 kA in a single null plasma configuration both in OH and NBI heated plasmas including H-mode plasmas.

2. EXPERIMENTAL SET-UP

Figure 1(a) shows a schematic drawing of the CT injector and the tokamak, including a TF coil position and a typical plasma configuration. The CT injector is installed perpendicularly to the magnetic axis on the midplane. The CT plasma is formed by the magnetized coaxial plasma gun

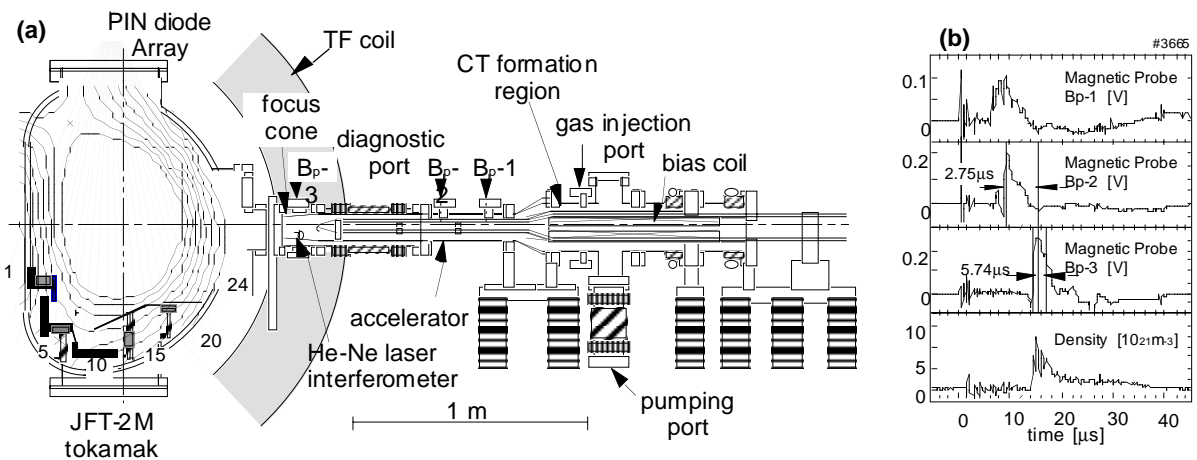


FIG. 1 (a) Cross-sectional view of the CT injector and the tokamak, including one TF coil position, typical plasma configuration and multi-chord PIN diode array (not same toroidal section). (b) Typical time evolution of signals of CT diagnostics. The CT injected into a plasma with $V_A=20 \text{ kV}$, $B_T=0.8 \text{ T}$.

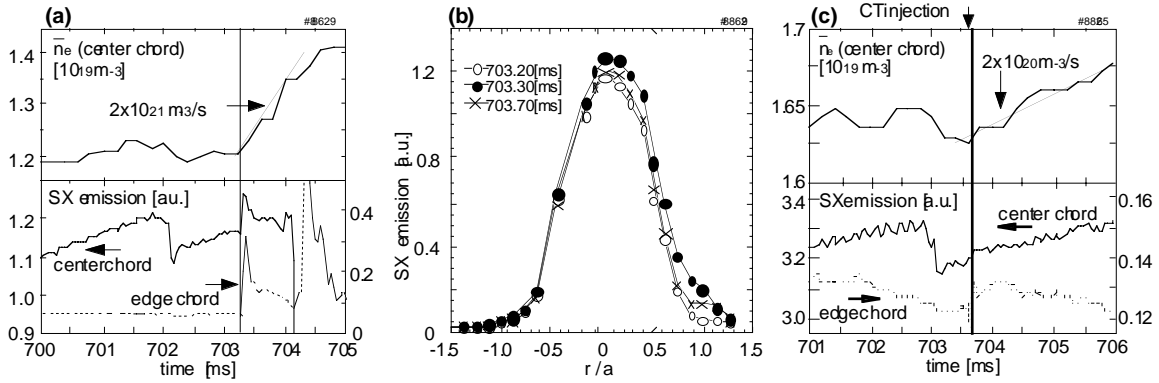


FIG. 2(a) Time behavior of the line-averaged electron density and the soft x-ray emission for the discharge with $B_T=0.8$ T, the CT injected at 703.25 ms. (b) Soft x-ray emission profile just before and after the CT injection. (c) Time behavior of the line-averaged electron density and the soft x-ray emission for the discharge with $B_T=1.3$ T, $I_p=240$ kA, the CT injected at 703.65 ms.

consisting of two coaxial electrodes and a bias solenoid. The plasma is pushed through the compressor by the intrinsic $\mathbf{J} \times \mathbf{B}$ force and accelerated in the second coaxial electrodes of 1 m long whose inner and outer diameters are 48 mm and 110 mm, respectively. These formation and acceleration electrodes are powered by capacitor banks of 20 kV (29 kJ) and 40 kV (74 kJ), respectively. In order to make the CT length short, the formation power supply is designed to have a very short rise time of 7 μ s. The CT is compressed to a diameter of 70 mm in the focus cone at the end of accelerator. Three magnetic pick-up probes along the outer electrode provide time-of-flight measurements to estimate the CT velocity and a helium-neon laser interferometer measures the density at the focus cone. A sample shot is shown in Fig. 1(b). In this case, the averaged velocity calculated from B_{p-2} and B_{p-3} , is relatively low about 110 km/s because of lower acceleration voltage and toroidal magnetic field. Maximum CT parameters obtained so far without toroidal field are n_{CT} (density) $\sim 9 \times 10^{21}$ m $^{-3}$, V_{CT} (velocity) ~ 300 km/s, B_{CT} (magnetic field) ~ 0.4 T. The injector is conditioned for several days by electrode bakeout under vacuum at 200°C before the injection experiments.

A multichord PIN diode array, shown in Fig. 1, measures soft x-ray emission profile with 50 μ s sampling time at 67.5° away from the CT injector. A fast response photodiode is mounted beside the CT injector port. A 130 GHz microwave interferometer measures the line averaged electron density with 0.2 ms sampling time along the horizontal center chord at the toroidal section 135° apart from the CT injector. Bolometer, D_α and electron cyclotron emission measurement systems are installed also in the microwave port.

3. EXPERIMENTAL RESULTS

3.1 CT injection into OH plasmas

A penetration depth of the CT into the tokamak magnetic field is determined by the balance between the kinetic energy of the CT and the toroidal magnetic field pressure[1]. A model calculation for JFT-2M tokamak predicts central penetration to the toroidal field $B_T=1$ T with the initial CT velocity 160 ± 20 km/s, density 5×10^{21} m $^{-3}$. We have observed central penetrations at $B_T=0.8$ T from soft x-ray emission profile measurements. Figure 2(a) shows the time trace of line-averaged electron density and soft x-ray emission for a discharge with $B_T=0.8$ T, $I_p=140$ kA, $q_s=2.95$, with the CT injection occurring at $t=703.25$ ms. The CT bank voltages for formation and acceleration are $V_F=17$ kV and $V_A=30$ kV, respectively. The averaged CT velocity calculated from the B_{p-1} and B_{p-3} time-of-flight is 185 km/s and the length is 0.26 m from the B_{p-3} signal width. The sharp rise of soft x-ray emission within 50 μ s was observed along the center chord as well as the edge chord and the electron density also increased rapidly at a rate of 2×10^{21} m $^{-3}$ /s just after the CT injection. The fuelling efficiency is roughly 20% from the increment of line-averaged electron

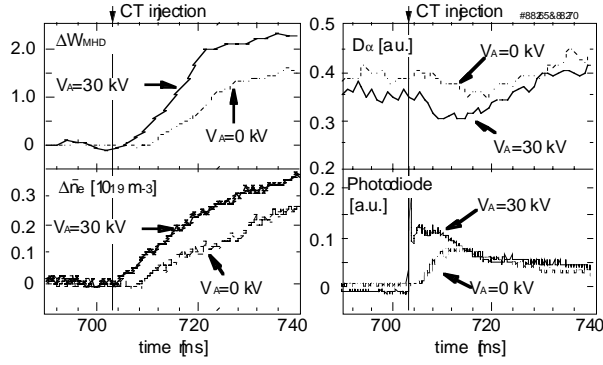


FIG. 3 Time behaviors of plasma parameters with $B_T=1.3$ T comparing $V_A=30$ kV (solid line) with $V_A=0$ kV (dashed line). The shot with $V_A=30$ kV is the same shot in Fig. 2(c) and $V_A=0$ is corresponding to the gas injection.

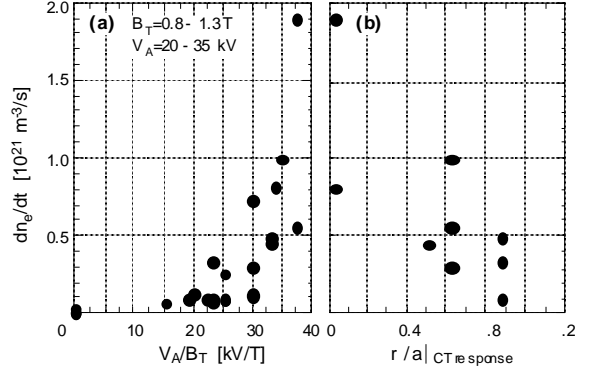


FIG. 4 Increase rate of the line averaged electron density in OH plasma against (a) CT acceleration voltage normalized by B_T , and (b) innermost soft x-ray channel position responding to CT injection.

density $\Delta \bar{n}_e \sim 0.2 \times 10^{19} \text{ m}^{-3}$ and the CT particle inventory $\sim 1.5 \times 10^{19}$. Figure 2(b) shows the change of the soft x-ray emission profile due to the CT injection, which is mostly related to the change of the electron density. Only outside channel intensities increased much and an asymmetrical profile is observed at $t=703.30$ ms. This increment of the outside channel intensity returns to the base level except some edge channels within 0.5 ms.

Central penetration of CT was not observed at $B_T=1.3$ T shown in Fig. 2(c). The peripheral soft x-ray chord at the position of $r/a \sim 0.9$ only increased at the CT injection and the density increase rate $2 \times 10^{20} \text{ m}^{-3}/\text{s}$ is an order less than that at $B_T=0.8$ T. Figure 3 shows the plasma parameters of the same shot shown in Fig. 2(c) with longer time scale. This shot is not accompanied by disruption and the stored energy W_{MHD} increased by 20 % after the CT injection. The data should be compared between discharges with and without acceleration voltage in order to discriminate the neutral gas effect diffused from the CT injector. A sharp pulse signal of the photodiode at the CT port shows the CT injection and the slow increase shows the effect of the diffusion gas in the $V_A=0$ kV case. For the $V_A=30$ kV case, the stored energy W_{MHD} increased about 2 kJ after the CT injection accompanied by decrease in D_α signal. The density dependence on W_{MHD} is roughly same in both cases. The effect of the diffused gas is dominant except first few ms just after the CT injection in this shallow penetration case.

Figure 4(a) shows the relation between the density increase rates and the CT acceleration voltage normalized by B_T . Since the CT penetration is determined by the balance between the CT kinetic energy and the toroidal magnetic pressure, this relation suggests that the density increase rate becomes larger with deeper CT penetration. Such a tendency is actually confirmed as shown in Fig. 4(b), where the horizontal axis indicates the innermost chord position of the soft x-ray array at midplane which detects a signal increase more than 5% from the base level, due to CT injection.

3.2 CT injection into H-mode plasmas with NBI heating

The CT injection was applied to an H-mode plasma produced by high power neutral beam injection and the central penetration was observed. Figure 5(a) shows a discharge with $B_T=0.8$ T, $P_{\text{NBI}}=1.2$ MW and $V_A=30$ kV. The averaged velocity of the CT is 160 km/s and the length is 0.28 m. The neutral beam injection started at $t=600$ ms, and L/H and H/L transitions were repeated from $t=630$ ms at each sawtooth crashes. The H-mode was maintained after $t=700$ ms and the CT was injected at $t=703.4$ ms. A sharp rise in the soft x-ray emissions both in center and edge channels and a rapid increase in the line-averaged electron density followed the CT injection, although the plasma was disrupted ~ 1 ms after the CT injection. The increment in electron density $0.2 \times 10^{19} \text{ m}^{-3}$ is similar as in the OH case in Fig. 2(a) but the increase rate is almost twice i.e. $\sim 4 \times 10^{21} \text{ m}^{-3}/\text{s}$. Contour plot of time evolution of the soft x-ray profile in Fig. 5(b) shows the CT penetrates into

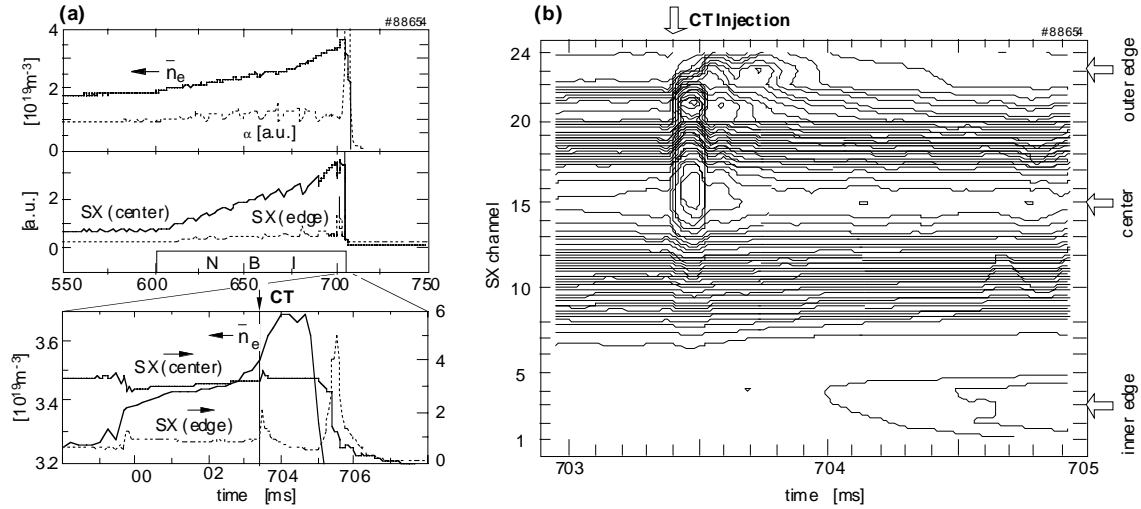


FIG. 5 (a) Time evolution of plasma parameters for the CT injection into H-mode plasma ($B_T=0.8$ T). (b) Soft x-ray emission contour showing the asymmetrical profile after the CT injection. Numbering of the SX channels is shown in Fig. 1.

the central region. The asymmetrical radial profile was kept for ~ 50 μ s and then suddenly disappeared without symmetrization. A second peak appeared in the outside edge channel and moved out with time. These behaviors in the soft x-ray profile suggest complexities of the CT dynamics in the tokamak plasma. There are possibilities of the toroidal rotation effect and/or the CT bouncing back from the central region, because the toroidal position of the PIN diode array is 67.5° away from the injection port. A reason of the disruption after CT injection has also not been well understood yet.

4. CONCLUSIONS

The CT injection experiments in NBI heated plasmas including H-mode were performed in the JFT-2M tokamak. It was demonstrated for the first time that the CT injected into the H-mode plasma penetrates into the central region with rapid increase in the electron density. The line-averaged electron density increased by $\Delta n_e \sim 0.2 \times 10^{19} \text{ m}^{-3}$ at a rate of $4 \times 10^{21} \text{ m}^{-3}/\text{s}$ in H-mode and $2 \times 10^{21} \text{ m}^{-3}/\text{s}$ in OH plasma. The fuelling efficiency is roughly 20%. The central penetration was obtained at $B_T=0.8$ T, while partial penetration in peripheral region was observed at $B_T=1.3$ T. The asymmetrical radial profile lasting for $\sim 50 \mu$ s was observed in the soft x-ray emission by the central CT penetration. Further study is needed to elucidate the reason of this behavior and the cause for disruption as well.

ACKNOWLEDGMENTS

Authors are grateful to Drs. H.Kishimoto, M.Ohta, A.Funahashi, M.Azumi and M.Shimizu for their continuous encouragement. The authors dedicate this paper to the memory of Dr. Norio Suzuki, who was the leader of JFT-2M group and passed away on 11 March 1998. He devoted his life to research of plasma physics and thermonuclear fusion.

REFERENCES

- [1] PERKINS, L.J., HO, S.K., HAMMER, J.H., Nuclear Fusion, 28 (1988) 1365.
- [2] MOLVIK, A.W., EDDLEMAN, J.L., HAMMER, J.H., et al, Phys. Rev. Lett. 66 (1991) 165.
- [3] RAMAN, R., MARTIN, F., QUIRION, B., et al., Phys. Rev. Lett. 73 (1994) 3101.
- [4] XIAO, C., et al., Fusion Energy 1996 (Proc. 16th Int. Conf. Montreal, 1996), Vol.1, IAEA, Vienna (1997) 595.
- [5] RAMAN, R., MARTIN, F., HADDAD, E., et al., Nuclear Fusion, 37 (1997) 967.
- [6] OGAWA, H., MIURA, Y., FUKUMOTO, N., et al, J. Nucl. Mater. 266-269 (1999) 623.